Multiple scattering model in GEANT4

L. Urbán
RMKI Research Institute for Particle and Nuclear Physics,
H-1525 Budapest, P.O. Box 49, Hungary and
CERN, CH-1211 Geneva 23, Switzerland

November 21, 2002

Abstract

We present a new multiple scattering (MSC) model to simulate the multiple scattering of charged particles in matter. This model does not use the Moliere formalism([Mol48]), it is based on the more complete Lewis theory ([Lew50]). The model simulates the scattering of the particle after a given step, computes the path length correction and the lateral displacement as well.

1 Introduction

The MSC simulation algorithms can be classified into two different classes, "detailed" and "condensed" simulation. In the detailed simulation all the collisions/interactions experienced by the particle are simulated. This simulation can be considered as exact, i.e. it gives the same results as the solution of the transport equation, but it can be used only if the number of collisions is not too large. This condition fulfils only if the kinetic energy of the particle is low enough or for special geometry (thin foil). For larger kinetic energies the average number of collisions are very large and the detailed simulation becomes very inefficient. The high energy simulation codes use condensed simulation algorithms, where the global effects of the collisions is simulated after a track segment. The global effects generally computed in these codes are the net displacement, energy loss and change of direction of the charged particle. These quantities are computed from the multiple scattering theories used in the codes. The accuracy ot these condensed simulations is limited by the approximations of the multiple scattering theories.

Most of the particle physics simulation codes use the multiple scattering theories due to Molière ([Mol48]), Goudsmit and Saunderson ([Goud40]) and Lewis ([Lew50]). The theories of Molière and Goudsmit-Saunderson give only the angular distribution after a step, while the Lewis theory computes the moments of the spatial distribution as well. None of the these MSC theories gives the probability distribution of the spatial displacement therefore each of the MSC simulation codes incorporates its own algorithm to determine the spatial displacement of the charged particle after a given step. These algorithms are not exact and they give the main uncertainties of the MSC codes. Therefore the simulation results can depend on the value of the step length and generally one has to select the "good" value of the step length carefully.

A new class of MSC simulation appeared in the literature recently, the "mixed" simulation algorithms (see e.g.[Fer93]). The mixed algorithm simulates the "hard" collisions one by one and uses a MSC theory to treate the effects of the "soft" collisions after a given step. The number of the steps can be kept not very large in these algorithms and the dependence on the step lenghth can be reduced, too.

The MSC model used in GEANT4 belongs to the class of the condensed simulations. The model is based on the Lewis' MSC theory. It uses model functions to determine the angular and spatial distributions after a step. The functions have been choosen in such a way that they give the same moments of the (angular and spatial) distributions than the Lewis theory.

2 The model

Let us define a few notations first.

The true path length ('t' path length) is the total length travelled by the particle. All the physical processes restrict this 't' step.

The geometrical (or 'z') path length is the straight distance between the starting and endpoint of the step, if there is no magnetic field. The geometry gives a constraint for this 'z' step. It should be noted, that the geometrical step length is meaningful in the case of magnetic field, too, but in this case it is a distance along a curved trajectory.

The properties of the multiple scattering process are completely determined by the transport mean free paths, λ_k, which are functions of the energy in a given material. The k-th transport mean free path is defined as

$$\frac{1}{\lambda_k} = 2\pi n_a \int_{-1}^{1} [1 - P_k(cos\chi)] \frac{d\sigma(\chi)}{d\Omega} d(cos\chi) \tag{1}$$

where $d\sigma(\chi)/d\Omega$ is the differential cross section of the scattering, $P_k(cos\chi)$ is the k-th Legendre polynomial, n_a is the number of atoms per volume.

Most of the mean properties of the MSC computed in the simulation codes depend on the first and second transport mean free paths only. The mean value of the geometrical path length (first moment) after a given true path length t is given by

$$< z >= \lambda_1 * (1. - e^{-\frac{t}{\lambda_1}}) \tag{2}$$

Eq. 2 is an exact result for the mean values of z, if the differential cross section has an axial symmetry and the energy loss can be neglected. This equation determines the transformation between the true and geometrical path length i.e. the so called path length correction. This formula and some other expressions for the first moments of the spatial distribution have been taken from [Fer93] or from [Kaw98], but the expressions have been calculated originally by Goudsmit and Saunderson [Goud40] and Lewis [Lew50].
If θ is the scattering angle after a true step length t, the mean value of $cos\theta$ is

$$< cos\theta >= e^{-\frac{t}{\lambda_1}} \tag{3}$$

The variance of $cos\theta$ can be written as

$$\sigma^2 =< cos^2\theta > - < cos\theta >^2 = \frac{1 + 2e^{-2\kappa\tau}}{3} - e^{-2\tau} \tag{4}$$

where $\tau = t/\lambda_1$ and $\kappa = \lambda_1/\lambda_2$.
The mean lateral displacement is given by a more complicated formula ([Fer93]), but this quantity also can be calculated relatively easily and accurately. The square of the mean lateral displacement is

$$< x^2 + y^2 >= \frac{4\lambda_1^2}{3} \left[\tau - \frac{\kappa + 1}{\kappa} + \frac{\kappa}{\kappa - 1} e^{-\tau} - \frac{1}{\kappa(\kappa - 1)} e^{-\kappa\tau}\right] \tag{5}$$

Here it is assumed that the initial particle direction is the direction of the axis z.
The transport mean free path values have been calculated by Liljequist et al. [Lil90], [Lil87] for electrons and positrons in the kinetic energy range 0.1 keV - 20 MeV in 15 materials. The MSC model uses these values with a linear interpolation or extrapolation of the transport cross section $\sigma_1 = 1/\lambda_1$ in the atomic number Z and in the square of the particle velocity β^2, when

it is necessary. The ratio κ is a very slowly varying function of the energy, it is above 2 for T bigger than few keV and it goes to 3 for very high energy (see [Kaw98]), so the constant value 2.5 is used in the model.

2.1 Path length correction

The path length correction in fact means here the transformation true path length $\Rightarrow$ geometrical path length and its inverse.
Given a true path length t the geometrical path length is sampled in the model according to the probability density function defined for $z \in [0, t]$

$$\begin{aligned} f(z) = & \quad [(k+1)/t]\ (z/z_0)^k & \text{for } z < z_0 \\ f(z) = & \quad [(k+1)/t]\ [(t-z)/(t-z_0)]^k & \text{for } z \geq z_0 \end{aligned} \tag{6}$$

As it can be seen $f(z)$ has a maximum at $z = z_0$. The value of z_0 depends on t, this dependence is approximated by the parametrization

$$z_0 =< z > +d\ (t- < z >) \tag{7}$$

where $< z >$ is the mean value of z, d is a constant model parameter.
The value of the exponent k is computed from the requirement that $f(z)$ should give the same mean value for z as eq. 2.

$$k = \frac{2 < z > -t}{z_0 - < z >} \tag{8}$$

The value of z is sampled according to $f(z)$ if $k > 0$, otherwise $z =< z >$ is used.
The geometrical path length $\Rightarrow$ true path length transformation is performed using the mean values

$$t = -\lambda_1 * log\left(1 - \frac{z}{\lambda_1}\right) \tag{9}$$

This transformation is needed when the particle arrives to a volume boundary and the step is limited by the geometry of the setup in terms of the geometrical path length. In this case the true path length should be computed in order to have the correct energy loss of the particle after the step.

2.2 Angle distribution

The quantity $u = \cos\theta$ is sampled according to a model function $g(u)$. The shape of this function has been choosen in such a way, that eqs. 3, 4 are satisfied. The functional form of this function is

$$g(u) = p[qg_1(u) + (1-q)g_3(u)] + (1-p)g_2(u) \tag{10}$$

where $0 \leq p, q \leq 1$, g_i are simple functions of $u = \cos\theta$ (normalized in $u \in [-1,\ 1]$). These functions have been chosen as

$$g_1(u) = C_1 \quad e^{-a(1-u)} \qquad -1 \leq u_0 \leq u \leq 1 \tag{11}$$

$$g_2(u) = C_2 \quad \frac{1}{(1-u)^c} \qquad -1 \leq u \leq u_0 \leq 1 \tag{12}$$

$$g_3(u) = C_3 \qquad -1 \leq u \leq 1 \tag{13}$$

where $a > 0$, $c > 0$ and u_0 are model parameters, C_i normalization constants. It is worth to note that for small scattering angle θ $g_1(u)$ is close to the Gaussian $exp(-\theta^2/2\theta_0^2)$ with $\theta_0^2 = 1/a$, while $g_2(u)$ has a Rutherford-like tail for large θ, if c is not far from 2 .

2.2.1 Determination of the model parameters

The parameters a, c, u_0 and p, q are not independent. It is required that the angle distribution function $g(u)$ and its first derivative should be continuous at $u = u_0$. These requirements gives 2 constraints for the parameters:

$$p\ g_1(u_0) = (1-p)\ g_2(u_0) \tag{14}$$

$$p\ a\ g_1(u_0) = (1-p)\ \frac{c}{1-u_0}\ g_2(u_0) \tag{15}$$

A third one comes from eq. 3, $g(u)$ should give the same mean value for u as the theory. A basic assumption of the model is, that the multiple scattering depends on the material and energy only via a dependence on the ratio $\tau = t/\lambda_1$.
It follows from eqs. 3 and 10 that

$$q\{p < u >_1 + (1-p) < u >_2\} = e^{-\tau} \tag{16}$$

where $< u >_i$ denotes the mean value of u computed from the distribution $g_i(u)$.
Two of the 5 parameters, a and u_0, have been chosen as independent. The other 3 can be computed from eqs. 14 - 16.All of the parameters depend on the variable τ, of course. For the parameter a the functional form $a(\tau) = \alpha(\tau)/\tau$ is assumed, where $\alpha(\tau)$ is a slowly varying function of τ, the main τ-dependence comes from the term $1/\tau$. This parametrization is in accordance with the parametrization used in the Highland-Lynch-Dahl formula

for the width of the angular distribution ([High75],[Lynch91]). The function $\alpha(\tau)$ has been parametrized as

$$\alpha(\tau) = \alpha_1 - \alpha_2 \ ln(\tau/\tau_0) \qquad \tau \leq \tau_0 \tag{17}$$

$$\alpha(\tau) = \alpha_1 + \alpha_3 \ ln(\tau/\tau_0) \qquad \tau \geq \tau_0 \tag{18}$$

α_i and τ_0 are some constants.The value of u_0 has been chosen as

$$u_0 = 1 - \xi/a \tag{19}$$

where ξ is a constant again. The numerical values of the parameters α_i and ξ have been determined from the comparison of the simulated angle distribution with experimental data. Here the experiment of Hanson et al.([Hans51]) has been used for the electron case, where the scattering of 15.7 MeV electrons has been measured on thin gold foils. For the multiple scattering of heavy particles, a part of the data set from [Gott93] has been used to determine the parameter values.(The same paramerized form describes both cases, only the values of α_i and ξ differ.) The numerical values can be found in the code. The data - simulation comparison for electrons can be seen in Fig.1.
It should be noted that in this model there is no step limitation originated from the multiple scattering process. Another important feature of this model is that the sum of the 'true' step lengths of the particle i.e. the total true path length does not depend on the length of the steps. Most of the algorithms used in simulations do not have these properties.
In the case of heavy charged particles ($\mu, \pi, proton, etc.$) the mean transport free path is calculated from the $e+/e-$ λ_1 values with a 'scaling': the transport mean free path λ_1 depends on the variable $P\beta$ only, where P is the momentum, β is the velocity of the particle.

In its present form the model samples the path length correction and angle distribution from some model functions while for the lateral displacement the mean value is used only and the correlations are neglected. However, the model is general enough to incorporate other random quantities and correlations in the future.

2.3 Nuclear size effects

The effect of the finite nuclear size is estimated in Born approximation ([Lil87]). In this very simple approximation the scattering cross section can be written as

$$\frac{d\sigma(\chi)}{d\Omega} = \frac{d\sigma_B(\chi)}{d\Omega} F(\chi) \tag{20}$$

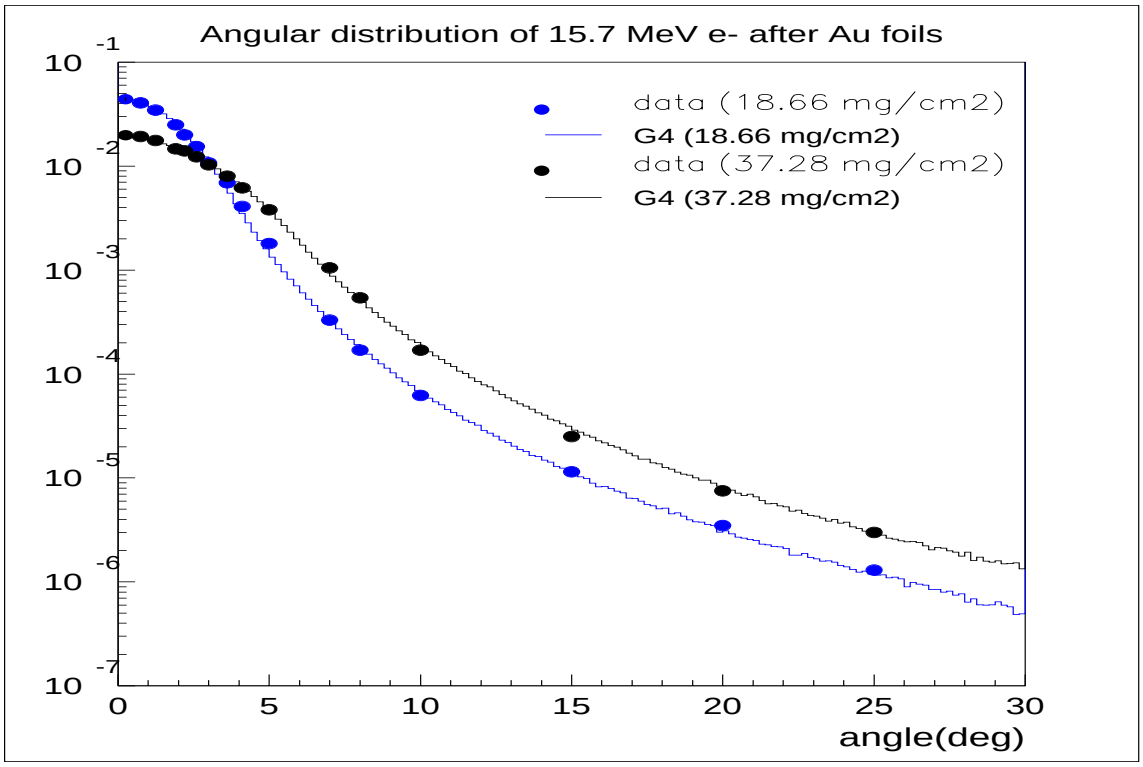

Figure 1: Angular distributions of 15.7 MeV electrons transmitted through gold foils, the data taken from [Hans51].

where $d\sigma_B/d\Omega$ is the Born cross section for a screened point-like nucleus and $F(\chi)$ is the squared nuclear form factor. $F(\chi) \approx 0$ if $\chi > \chi_{max}$ where

$$sin(\frac{\chi_{max}}{2}) = \frac{1}{kR} \tag{21}$$

where k is the particle wave number and R is the nuclear radius. This correction means that $\sigma(\chi)$ decreases, so λ_1 defined by

$$\frac{1}{\lambda_1} = 2\pi n_a \int_{cos\chi_{max}}^{1} [1 - P_1(cos\chi)] \frac{d\sigma_B(\chi)}{d\Omega} F(\chi) d(cos\chi) \tag{22}$$

increases for larger energies.

3 MSC simulation in GEANT4

The step length of the particles is determined by the physics processes or the geometry of the detectors. The tracking/stepping algorithm checks all the step lengths demanded by the (continuous or discrete) physics processes and determines the minimum of these step lengths. This minimum step length then should be compared with the length determined by the geometry of the detectors and one has to select the minimum of the 'physics step length' and the 'geometrical step length' as the actual step length. This is the point where the MSC model comes into the game first. All the physics processes 'feel' the true path length t travelled by the charged particle while the step limitation originated from the geometry is a geometrical path length z. The MSC algorithm transforms the 'physics step length' into a 'geometrical step length' before the comparison of the two lengths. This 't'⇒'z' transformation can be called as the inverse of the path length correction . After the actual step length has been determined and the particle relocation has been performed the MSC performs the transformation 'z'⇒'t', because the energy loss and scattering computation need the true step length 't'.

The scattering angle θ of the particle after the step of length 't' is sampled according to the model function given in eq. 10 . The azimuthal angle ϕ is generated uniformly in the range $[0, 2\pi]$.

After the simulation of the scattering the lateral displacement is computed using eq. 5. Before doing this a check is performed to ensure that the relocation of the particle with the lateral displacement does not take the particle beyond the volume boundary.

3.1 Boundary crossing algorithm

In GEANT4 the boundary crossing is treated by the transportation code/process ([GEANT4]). The transportation ensures that the particle does not penetrate in a new volume without stopping at the boundary, it restricts he step size when the particle leaves a volume. However, there is no similar step limitation when a particle enters a volume and this fact does not allow a good backscattering simulation for low energy particles. Low energy particles penetrate deeply into the volume in the very first step and then -because of energy loss- they are not able to reach again the boundary in backward direction.

A very simple boundary crossing algorithm has been implemented in the MSC code to cure this situation. Entering in a new volume the algorithm restricts the step size to a value $f_r \cdot max\{r, \lambda\}$, where r is the range of the particle, f_r is a constant ($f_r \in [0, 1]$). It can be easily seen that this kind of step limitation means a real contraints for low energy particles only. The choice of the parameter f_r is a question related with performance. By default $f_r = 0.2$ is used as a compromise between performance and physics, but this parameter can be set to any other value in a simple way. One can get an approximate simulation of the backscattering with the default value, while if a better backscattering simulation is needed it is possible to get it using a small value for f_r.

4 Comparison with experimental data

In this section some benchmark comparisons are presented, mainly with experiments deal with electron beams impinging normally on different materials. The comparison with data of Hanson et al. ([Hans51]) is not a real benchmark, because these data were used to tune the model parameters.

In Fig.2 the lateral spreading of a 2.5 MeV proton beam is shown after mylar foils of different thicknesses. The spreading is measured in a distance 6.3 mm after the foils, the line representing the experimental data have been taken from [Mich01], the squares are the simulation results. The lateral spreading of the beam is directly connected with the angle distribution of the beam after the mylar absorber, so this result is a benchmark comparison for the angle distribution.

Fig. 3 shows the number transmission coefficient T as function of the foil thickness for 1 MeV electrons in aluminium. The thickness is measured in

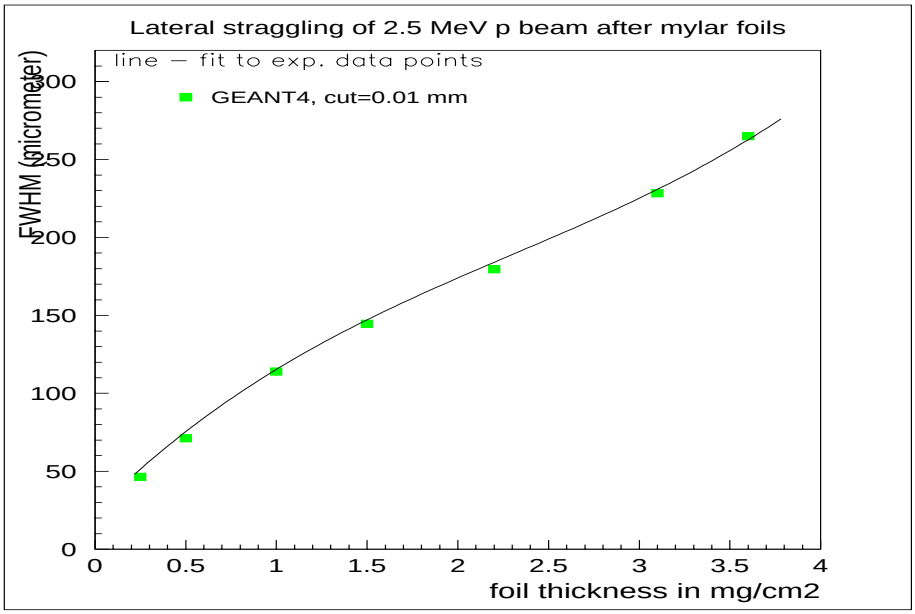

Figure 2: Lateral spreading of a 2.5 MeV proton beam after mylar foils, the data from [Mich01].

units of the continuous slowing down range, the data originated from different measurements have been taken from the review paper of Seltzer and Berger ([Selt74]). Here two simulation results are shown with different production cuts, for cut value of 10 mm (4.5 MeV in energy) there are no secondaries, while for 1 keV ($1\mu m$) cut there are a great number of delta electrons. The simulated transmission coefficients are slithly small using 10 mm cut, but the simulation with small cut reproduces the data quite well.

The next benchmark comparison in Fig. 4 gives the energy deposit distribution of 0.5 MeV electrons in aluminium as a function of depth (depth-dose distribution). The experimental points have been taken from [Selt74], the simulation agrees with the data within errors.

The energy spectra of 1 MeV electrons transmitted through aluminium foils is shown in Fig. 5. The experimental points are from a measurement of Rester and Derrickson ([Rest71]). The simulation again are quite close to the data.
Some backscattering results are shown in Figs 6. and 7. which demonstrate the need for the boundary crossing algorithm. In Fig. 6 the backscattering coefficients for 35 keV positrons backscattered from thick gold target are compared with experimental data of Coleman et al. ([Cole92]). The 3 simu-

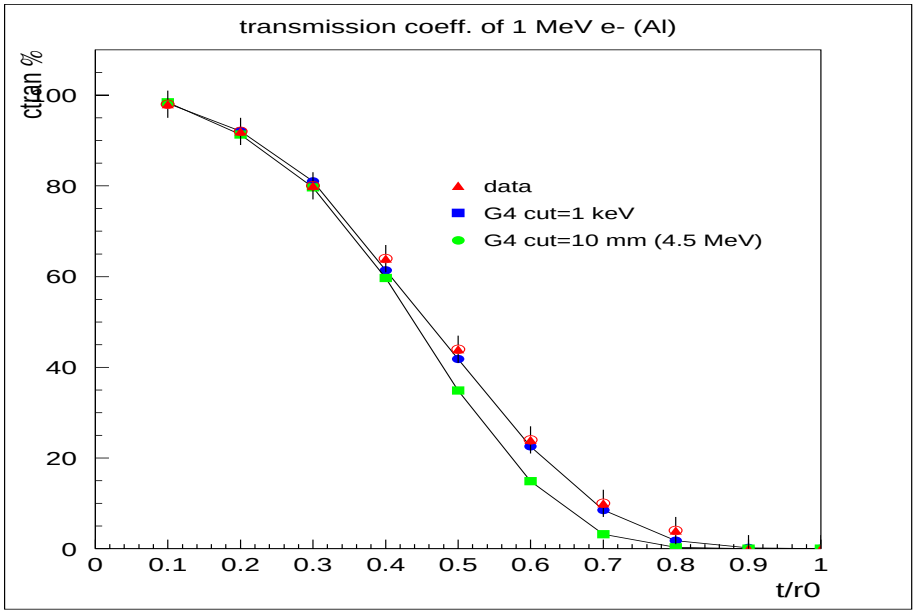

Figure 3: Number transmission coefficients T in aluminium for 1 MeV e^-, the data from [Selt74].

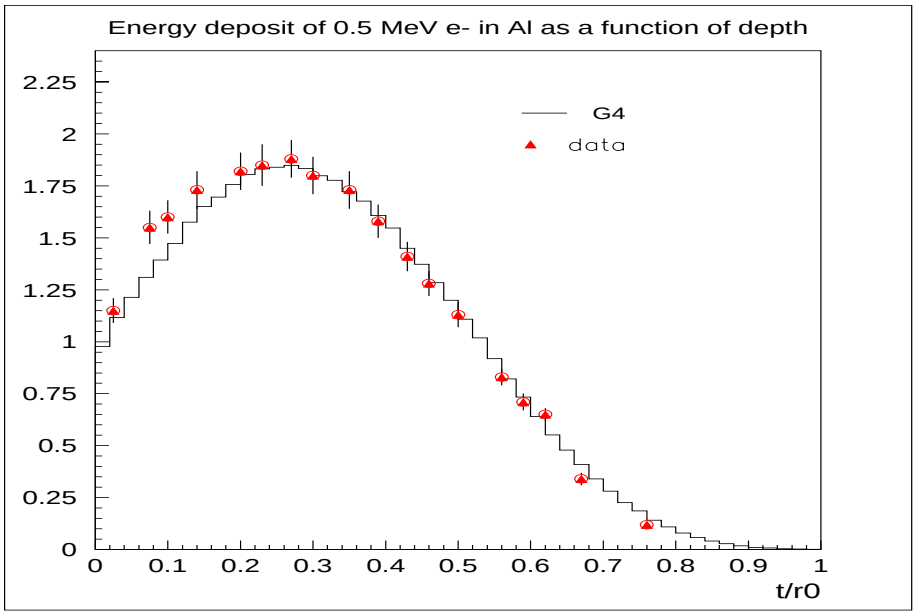

Figure 4: Energy deposit distribution of 0.5 MeV electrons in aluminium as a function of depth, the data from [Selt74].

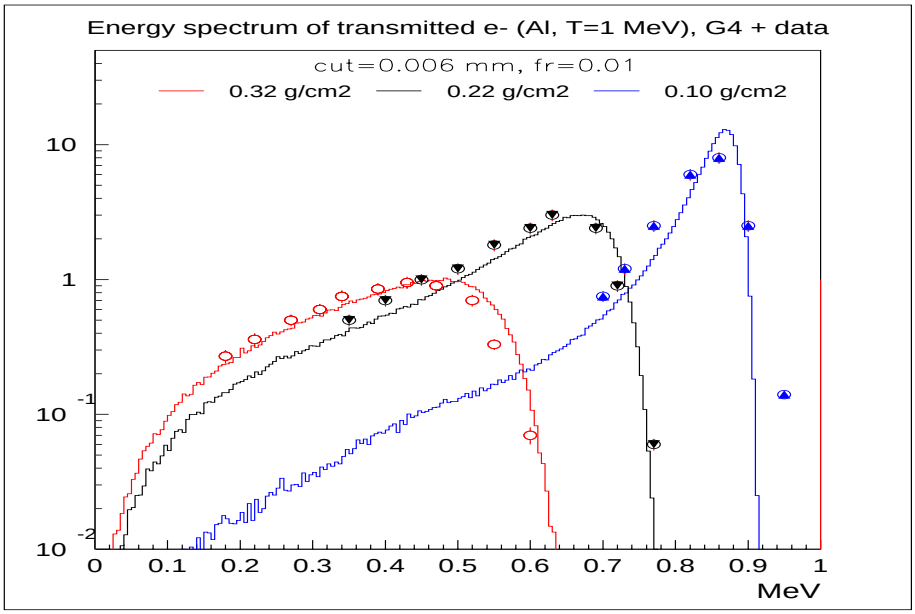

Figure 5: Energy specrum of 1 MeV electrons transmitted through aluminium layers, the data from [Rest71].

lation results from the bottom to the top has been computed with $f_r = 1$ (i.e. without the boundary crossing algorithm), with $f_r = 0.1$ and with $f_r = 0.01$. It can be seen that the backscattering is not reproduced without the algorithm and the simulation is close to the data when the value of f_r becomes small.

The Monte Carlo/data ratios are plotted in Fig. 7 with different values of f_r for 3 different cases : 40 keV e^-, carbon absorber, 35 keV e^+ on gold and 2 MeV e^- on copper. The ratio goes to 1 for all of the cases with decreasing f_r. Without the boundary crossing algorithm (i.e. $f_r = 1$) the backscattering simulation results differ significantly from the data for low energy particles, while at higher energy the backscattering simulation is better even in this case.

5 Conclusions

A new multiple scattering model hes been implemented in GEANT4. Despite its simplicity the model is capable to describe the mean properties of the multiple scattering process and reproduce the experimental results well.

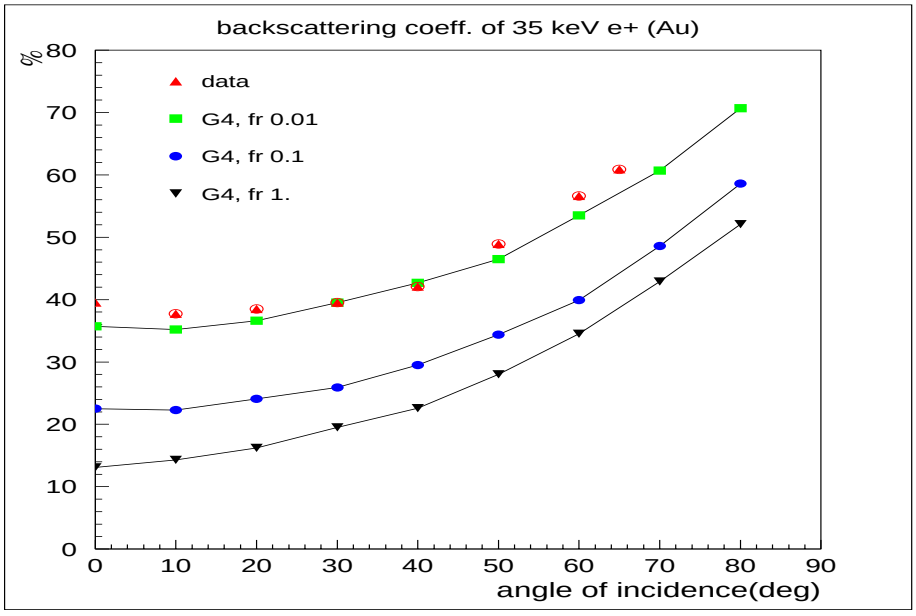

Figure 6: Backscattering coefficients of 35 keV positrons from thick gold target as a function of angle of incidence, the data are from [Cole92].

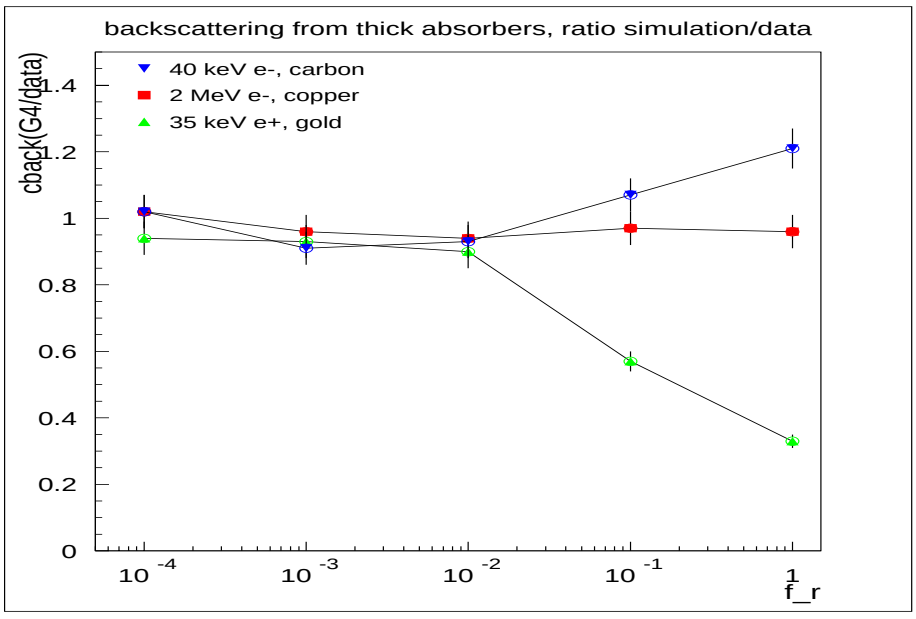

Figure 7: Backscattering from thick absorbers, G4/data as a function of parameter f_r

6 Acknowledgement

I am indebted to M. Maire for enlightening discussions and for his criticism reading the manuscript. I would like to thank the API group of IT (CERN) for the support.

References

[GEANT4] GEANT4 collaboration *http://geant4.web.cern.ch/geant4/*

[Mol48] *Z. Naturforsch. 3a (1948) 78.*

[Fer93] J. M. Fernandez-Varea et al. *NIM B73 (1993) 447.*

[Goud40] S. Goudsmit and J. L. Saunderson. *Phys. Rev. 57 (1940) 24.*

[Lew50] H. W. Lewis. *Phys. Rev. 78 (1950) 526.*

[Kaw98] I. Kawrakow and Alex F. Bielajew *NIM B 142 (1998) 253.*

[Lil87] D. Liljequist and M. Ismail. *J.Appl.Phys. 62 (1987) 342.*

[Lil90] D. Liljequist et al. *J.Appl.Phys. 68 (1990) 3061.*

[High75] V.L.Highland *NIM 129 (1975) 497.*

[Lynch91] G.R. Lynch and O.I. Dahl *NIM B58 (1991) 6.*

[Hans51] A. O. Hanson et al. *Phys. Rev. 84 (1951) 634.*

[Gott93] B.Gottschalk et al. *NIM B74 (1993) 467.*

[Mich01] C. Michelet et al. *NIM B 181 (2001) 157.*

[Selt74] S. M. Seltzer and M. J. Berger *NIM 119 (1974) 157.*

[Rest71] D. H. Rester and J. H. Derrickson *J. Appl. Phys. 42 (1971) 714.*

[Cole92] P.G. Coleman et al. *J.Phys: Condens.Matter 4 (1992) 1031.*